

Jet correlation measurement in heavy-ion collisions: from RHIC to LHC

Constantinos A. Loizides

Massachusetts Institute of Technology, 77 Mass Ave, Cambridge, 02139, MA, USA

E-mail: loizides@mit.edu

Abstract. We attempt to deduce simple options of ‘jet quenching’ phenomena in heavy-ion collisions at $\sqrt{s_{NN}} = 5.5$ TeV at the LHC from the present knowledge of leading-hadron suppression at RHIC energies. In light of the nuclear modification factor for leading particles we introduce the nuclear modification factor for jets, R_{AA}^{jet} , and for the longitudinal momenta of particles along the jet axis, R_{AA}^{pL} .

1. Introduction

At RHIC energies, hard probes, mainly light quarks and gluons, are experimentally accessible in heavy-ion collisions with sufficiently high rates. Their production is quantified using inclusive single-particle spectra at high momentum ($p_T > 2 - 3$ GeV). The suppression of these high-momentum (leading) particles in central nucleus–nucleus relative to peripheral or pp collisions is one of the major discoveries at RHIC. In Au–Au collisions at various centre-of-mass energies ($\sqrt{s_{NN}} = 62.4, 130$ and 200 GeV) the two experiments with high transverse-momentum capabilities, PHENIX and STAR, but also PHOBOS and BRAHMS, have measured:

- the suppression of single-particle yields at high p_T ($\gtrsim 2 - 4$ GeV) [1–5];
- the disappearance, in central collisions, of jet-like correlations in the azimuthally-opposite side (away-side) of a high- p_T leading particle [6, 7] and, quite recently, the reappearance of the particles on the away-side manifested in low-momentum hadrons [8, 9];

The absence of these effects in d–Au collisions at the same centre-of-mass energy ($\sqrt{s_{NN}} = 200$ GeV) [1, 10–12] confirms that in (central) nucleus–nucleus collisions final-state (as opposed to initial-state) effects modify the measured particle spectra.

The experimental observations have been explained in terms of various quenching models, where the energetic partons produced in the initial hard scattering ‘lose’ energy as a consequence of the interaction with the dense, partonic matter. Most models implement parton energy loss according to medium-induced gluon radiation of a hard parton traversing dense partonic matter of finite size [13–21]. Also hadronic interactions [22, 23] have been investigated and partially found to contribute to the observed depletion of the hadron spectra.

At the LHC at 30 times higher centre-of-mass energy, hard probes will be abundantly produced, even at energies of more than one order of magnitude higher than at RHIC. These energetic partons might be identified by their fragmentation into hadronic jets of high energy. In contrast with RHIC, the initial energy of $E_T > 50$ GeV is high enough to allow the full reconstruction of the hadronic jet, even in the underlying heavy-ion environment [24]. Therefore, measurements of changes in the properties of identified jets in nucleus–nucleus with respect to pp collisions will become possible.

In the present work we attempt to deduce perspectives for ‘jet quenching’ measurements at LHC given present data and models of hadron suppression at RHIC. In section 2 we introduce PQM, a model that describes high- p_T suppression at RHIC, and state its prediction of the nuclear modification factor for LHC. In section 3 we argue that the surface-emission effect limits the sensitivity of leading particles to the density of the medium. In section 4 we present a PYTHIA simulation of jet quenching at LHC conditions and introduce the nuclear modification factor for identified jets, R_{AA}^{jet} , and for the longitudinal momenta of particles along the reconstructed jet axis, R_{AA}^{pL} .

2. Leading-particle spectroscopy at RHIC and LHC conditions

The effect of the medium on the production of a hard probe is typically quantified via the nuclear modification factor,

$$R_{AB}(p_T, \eta; b) = \frac{1}{\langle N_{\text{coll}}(b) \rangle} \times \frac{d^2 N_{AB}^{\text{hard}} / dp_T d\eta}{d^2 N_{pp}^{\text{hard}} / dp_T d\eta}, \quad (1)$$

which measures the deviation of the nucleus–nucleus from the superposition of independent nucleon–nucleon collisions. In absence of strong nuclear initial-state effects it should be unity, if binary collision scaling holds.

Figure 1 (left) shows $R_{AA}(p_T)$ for central Au–Au collisions at $\sqrt{s_{NN}} = 200$ GeV as published by PHENIX [3, 4] and STAR [2] together with a pQCD calculation of parton energy loss obtained with our Monte Carlo program PQM (Parton Quenching Model) [20].

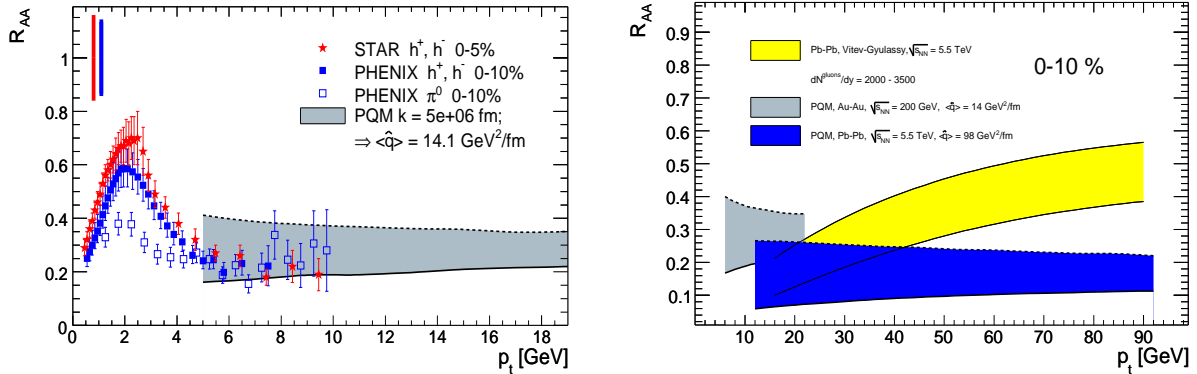


Figure 1. Left: $R_{AA}(p_T)$ for central Au–Au collisions at $\sqrt{s_{NN}} = 200$ GeV. PHENIX [3, 4] and STAR [2] data are reported with combined statistical and p_T -dependent systematic errors (bars on the data points) and p_T -independent systematic errors (bars at $R_{AA} = 1$). The theoretical calculation is obtained with PQM resulting in an average transport coefficient of $14 \text{ GeV}^2/\text{fm}$. The band denotes the systematical uncertainty of the model. Right: The PQM prediction for $R_{AA}(p_T)$ in central Pb–Pb collisions at $\sqrt{s_{NN}} = 5.5$ TeV. The LHC prediction presented in Ref. [17] (Vitev–Gyulassy) and PQM for central Au–Au collisions at RHIC, $\sqrt{s_{NN}} = 200$ GeV, are shown for comparison.

PQM combines a recent calculation of the BDMPS-Z-SW parton energy loss [25] with a realistic description of the collision geometry at mid-rapidity. Our approach allows to calculate the transverse momentum and centrality dependence of single- and di-hadron correlation suppression, as well as the ‘energy-loss induced’ azimuthal anisotropy of particle production in non-central collisions. The model has one single parameter, k , that sets the scale of the density of the medium. Once the parameter is fixed, e.g. on the basis of the nuclear modification data at $\sqrt{s_{NN}} = 200$ GeV, we scale it to different energies and collision systems assuming its proportionality to the expected volume-density of gluons. The application of our model is restricted to the high- p_T region, above $4 - 5$ GeV at RHIC and above 10 GeV at LHC energies, since we do not include initial-state effects.

The leading-particle suppression in nucleus–nucleus collisions is obtained by evaluating

$$\left. \frac{d^2\sigma_{\text{quenched}}^h}{dp_T d\eta} \right|_{\eta=0} = \sum_{a,b,j=q,\bar{q},g} \int dx_a dx_b d\Delta E_j dz_j f_a(x_a) f_b(x_b) \left. \frac{d^2\hat{\sigma}^{ab\rightarrow jX}}{dp_{t,j}^{\text{init}} d\eta_j} \right|_{\eta_j=0} \times \delta(p_{t,j}^{\text{init}} - (p_{t,j} + \Delta E_j)) P(\Delta E_j; R_j, \omega_{c,j}) \frac{D_{h/j}(z_j)}{z_j^2}, \quad (2)$$

in a Monte Carlo approach. Equation (2) describes the production of high- p_T hadrons within the perturbative QCD collinear factorization framework, at mid-rapidity, $\eta = 0$, including medium-induced parton energy loss in the BDMPS-Z-SW formalism. $f_{a(b)}$ is the parton distribution function for a parton of type $a(b)$ carrying the momentum fraction $x_{a(b)}$, $\hat{\sigma}^{ab\rightarrow jX}$ is the partonic hard-scattering cross sections and $D_{h/j}(z_j)$ is the fragmentation function, i.e. the probability distribution for the parton j to fragment into a hadron h with transverse momentum $p_T = z_j p_{t,j}$. The modification with respect to the pp (vacuum) case is given by the energy-loss probability, $P(\Delta E_j; R_j, \omega_{c,j})$, for the parton j . Its two input parameters, the kinematical constraint and the characteristic scale of the radiated gluons, depend on the in-medium path length L of the parton and on the BDMPS transport coefficient of the medium, \hat{q} . The latter is defined as the average medium-induced transverse momentum squared transferred to the parton per unit path length. (See Ref. [20] on how we calculate the two parameters R and ω_c for a given parton and realistic geometry.) In the original calculation [25], the energy-loss probability (quenching weight) is independent of the energy of the original parton allowing a parton with finite energy to radiate more than its energy. To account for finite parton energies we have introduced two different ways of constraining the weights, the *non-reweighted* and *reweighted* case. In the first case we constrain the loss to the energy of the parton, whenever the radiated energy is determined to be larger than that. In the second case we require by truncation of the distribution that the energy loss is less than the energy of the parton. The resulting energy loss is larger in the *non-reweighted* case, because partons ‘thermalize’ with a probability $\int_E^\infty d\epsilon P(\epsilon)$. It is argued [21, 25] that the difference in the values of the observables for the two approaches illustrates the theoretical uncertainties of the model.

Coming back to fig. 1 (left) we note that for the chosen value of k the calculation reproduces $R_{AA}(p_T)$ for central Au–Au collisions at $\sqrt{s_{NN}} = 200$ GeV. In Ref. [20] we consistently compare model predictions to various high- p_T observables at RHIC energies. We also show that we need to scale k by a factor of seven to obtain the LHC prediction of R_{AA} at $\sqrt{s_{NN}} = 5.5$ TeV shown in fig. 1 (right). Our prediction for the LHC is in agreement, both in the numerical value and in the p_T -dependence, with that obtained in Ref. [21], while it is quite different from the one calculated in Ref. [17].

3. Properties of leading-hadron suppression

At LHC energies, the expected R_{AA} for central Pb–Pb collisions at LHC as a function of p_T is rather flat, i.e. almost p_T -independent, similar to what is observed at RHIC at $p_T > 4$ GeV. To study this p_T -dependence we show in fig. 2 $R_{AA}(p_T)$ in central Pb–Pb at LHC for $\langle \hat{q} \rangle = 12$ GeV²/fm (corresponding to the value found at RHIC), $\langle \hat{q} \rangle = 24$ GeV²/fm and $\langle \hat{q} \rangle = 98$ GeV²/fm (the value obtained by the scaling from RHIC to LHC), as well as the result of a calculation with fixed $\hat{q} = 10$ GeV²/fm and fixed length of 4.4 fm. Clearly, the fixed-length calculation shows a stronger p_T -dependence than the PQM calculation.

As we explain in the following, the flatness of R_{AA} is a consequence of

- the steeply falling production cross-section, $\propto \left(\frac{1}{p_T^{\text{hadron}}} \right)^{n(p_T)}$, where $n(p_T)$ is rising from about 7 to 12 (RHIC) and from 6 to 7 (LHC) in the relevant p_T regime;
- the emission from the surface, which for large medium densities dominates [26].

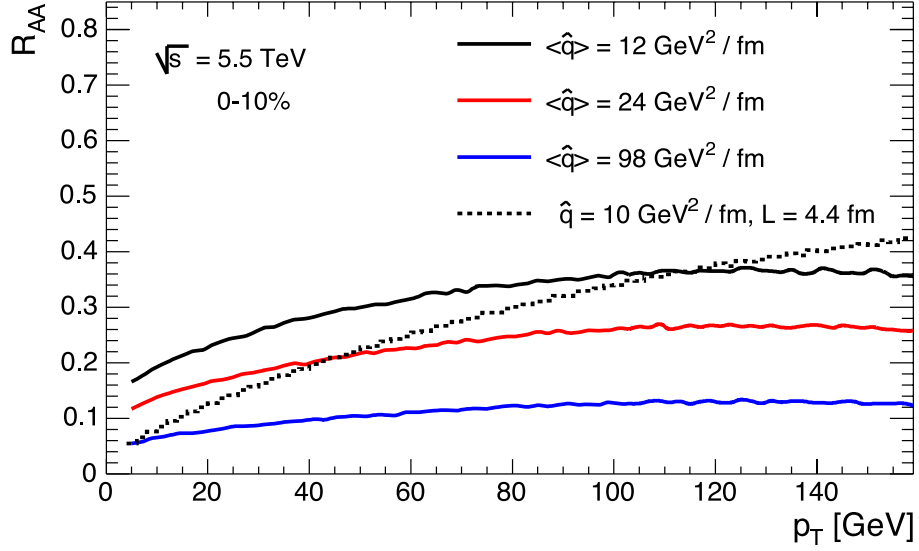


Figure 2. R_{AA} as a function of p_T for 0–10% most central collisions at LHC energy obtained by PQM. The calculations in the parton-by-parton approach (solid lines) are compared to a calculation for fixed transport coefficient and length (dashed). All graphs are in the non-reweighted case.

R_{AA} , eq. (1), at mid-rapidity, can be approximated by

$$R_{AA}(p_T) = \int d\Delta E P(\Delta E, p_T + \Delta E) \frac{dN^{PP}(p_T + \Delta E)}{dp_T} \bigg/ \frac{dN^{PP}(p_T)}{dp_T}, \quad (3)$$

where, dN^{PP}/dp_T is the spectrum of hadrons (or partons) in the case of no medium (i.e. pp neglecting initial state effects). The suppression computed with eq. (3) is found to give a rather good approximation to the one computed with PQM or with the full formula, eq. (1). In the case the production spectrum is (approximately) exponential the p_T -dependence cancels in the ratio and we find R_{AA} to be (approximately) independent of p_T . At RHIC this is the case at about $p_T \geq 30$ GeV. Below that value and at the measured values of 5–12 GeV, as well as at the LHC ($n(p_T) \leq 7$), the spectrum is given by a power-law. It was expected [27] that $R_{AA} \propto (1 + c/\sqrt{n(p_T)p_T})^{-n(p_T)}$, i.e. reaching unity for large p_T .

However, this neglects the fact that for dense media surface emission or, more generally, the probability to have no energy-loss, $P(\Delta E = 0, E)$, plays a significant role, an effect which is even more pronounced at low p_T (compared to ω_c). To simplify our argumentation we allow either no loss ($\Delta E = 0$) or complete loss ($\Delta E = E$) in the non-reweighted case, $P(\Delta E, E) = p_0 \delta(\Delta E) + (1 - p_0) \delta(\Delta E - E)$.¹ Inserting the constrained weight into eq. (3) we obtain

$$R_{AA}(p_T) = p^* + (1 - p^*) \frac{dN^{PP}(2p_T)}{dp_T} \bigg/ \frac{dN^{PP}(p_T)}{dp_T}. \quad (4)$$

It is obvious that eq. (4) is just a crude approximation, but it demonstrates that the value of R_{AA} is dominated by the fraction of hadrons (or partons), which escape without losing much of their energy. For the simple power-law production spectrum the contribution from higher p_T is suppressed by about $(1 + \Delta E/p_T)^{n(p_T)}$. Taking into account only fixed values of \hat{q} and L the probability p^* is given by the discrete weight, p_0 , at $R = 0.5 \hat{q} L^3$, amounting to about 0.05(0.002) for quarks(gluons). However, for a

¹ For a dense medium the constrained weights at low parton energy indeed do have a sharp peak at zero and at maximum possible energy loss, whereas the values in between are negligible.

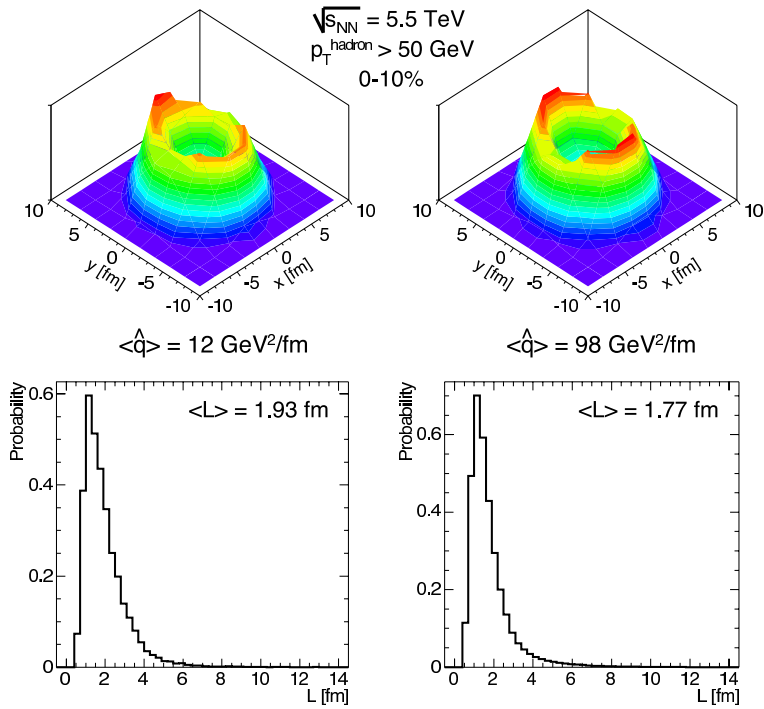


Figure 3. Distributions of parton production points in the transverse plane (upper row) and in-medium path length (lower row) for partons that escape the medium and produce hadrons with $p_T > 50$ GeV in central Pb–Pb collisions at 5.5 TeV for $\langle \hat{q} \rangle = 12 \text{ GeV}^2/\text{fm}$ (left) and $\langle \hat{q} \rangle = 98 \text{ GeV}^2/\text{fm}$ (right). The quantity $\langle L \rangle$ denotes the average of the path-length distribution. The calculation is for the non-reweighted case.

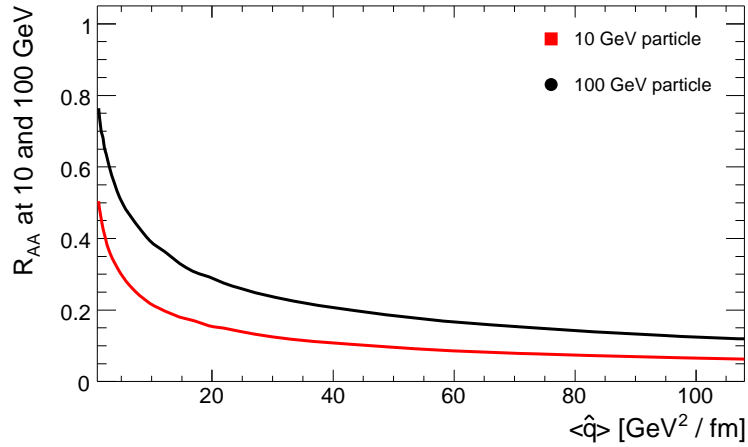


Figure 4. R_{AA} as a function of the average transport coefficient, $\langle \hat{q} \rangle$, for 10 and 100 GeV hadrons in 0–10% central Pb–Pb collisions at $\sqrt{s_{NN}} = 5.5$ TeV. The calculation is for the non-reweighted case.

proper calculation one must take into account the right production ratio of quarks-to-gluons. For realistic path-length distributions p^* is dominated by partons, which are emitted close to the surface and, thus, enhanced relative to p_0 obtained at fixed scale. It turns out that p^* evaluated with PQM at LHC central

conditions, averaged over path-lengths and parton types, is independent of p_T in the range shown above, and takes values of about 0.14, 0.1 and 0.05 for the scales used in fig. 2.

Surface emission will be present even for very large-momentum hadrons. Figure 3 (top) visualizes the distribution of production points (x_0, y_0) in the transverse plane for partons, which escape from the dense overlap region and yield hadrons with $p_T^{\text{hadron}} > 50$ GeV. The chosen values of the medium density correspond to the value found at RHIC and the expectation for LHC. The corresponding in-medium path-length distributions, fig. 3 (bottom), reveal that the average ‘thickness’ of the emission surface is restricted to less than 2 fm: even hadrons with $p_T > 50$ GeV are emitted dominantly from the surface.

The dominance of the surface effect limits the sensitivity of leading particles to the density of the medium, mainly for experimentally accessible low- p_T range at RHIC. This is demonstrated in fig. 4 where we show the dependence of R_{AA} on the average transport coefficient evaluated with PQM for 0–10% most central collisions at $\sqrt{s_{NN}} = 5.5$ TeV first shown in Ref. [21]. For 10 GeV hadrons the nuclear modification factor is sensitive to average medium densities up to about 15 GeV²/fm, and for 100 GeV hadrons the sensitive regime might widen to average values of about 30.

4. Jet spectroscopy and modification of jet properties

At LHC, leading-hadron spectroscopy will be naturally extended by jet spectroscopy. Simulations show that jets with transverse energies of more than 50 GeV are identifiable and reconstructible on an event-by-event basis, even in most central collisions; however with severe limitations in the resolution of the jet energy. The interaction of the hard partons with the medium created in these collisions is expected to manifest in the modification of jet properties deviating from known fragmentation processes in vacuum. Calculations predict that the additional gluons radiated by the original parton remain (fragment) inside the jet cone, although redistributed in transverse phase space [25, 28]. The corresponding jet-production cross section is expected to follow binary scaling. However, the jet shape is claimed to broaden and the jet multiplicity to soften and increase [29]. Ideally, if one reconstructs the hadronic energy for outstanding high-energy jets the jet energy may be associated with the original energy of the parton.

In combination with results at lower parton energies from correlation methods jet measurements at higher energy might complete the picture of medium-induced parton-energy-loss phenomena. In the following it is our aim to introduce a simulation and analysis of jet quenching effects. Details can be found in Ref. [24]. Unquenched jets representing the pp reference are generated using the PYTHIA generator [30]. Quenched signal jets are simulated as an afterburner to PYTHIA developed by A. Morsch. It introduces parton energy loss via final-state gluon radiation, in a rather ad-hoc way: Before the partons originating from the hard 2-to-2 process (and the gluons originating from ISR) are subject to fragment, they are replaced according

$$\text{parton}_i(E) \rightarrow \text{parton}_i(E - \Delta E) + n(\Delta E) \text{gluon}(\Delta E/n(\Delta E))$$

conserving energy and momentum. For each parton, ΔE is calculated by PQM in the non-reweighted case and depends on the medium density, parton type and parton production point and emission angle in the collision overlap region. The number of radiated gluons, $1 \leq n(\Delta E) \leq 6$, is determined by the condition that each gluon must have less energy than the quenched parton from which it was radiated away. First results using this afterburner at LHC energies have been discussed in Ref. [31].

For the following sample analysis we have prepared events containing jets simulated with the modified PYTHIA version for $\langle \hat{q} \rangle = 1.2, 12$ and 24 GeV²/fm, which are embedded into 0–10% central HIJING [32] events. The choice of first value implies only a very little modification of the embedded quenched jets compared to embedding of jets with standard PYTHIA. The second corresponds to the case found to describe the R_{AA} at RHIC, whereas the third is a conservative choice about a factor of four smaller than the expected value extrapolated from RHIC to LHC.

The jet finding is based on final particles (no detectors effects) at mid-rapidity ($-1 < \eta < 1$). We use the standard ILCA cone finder [33]. However, to cope with the soft heavy-ion background we need

restrict the cone radius to $R = 0.3$. For charged particles we require $p_T \geq 2$ GeV. The same settings are used for the reference jet measurement in pp. In central Pb–Pb collisions the mean reconstructed jet energy is about 80% for 50 GeV jets, and more than 90% for 100 GeV jets; the resolution is about 20% and 10%, respectively.

4.1. Nuclear modification factor for jets

It has been shown [29] that the medium-induced broadening of the jet reduces the energy inside $R = 0.3$ by $\sim 15\%$ and by $\sim 7\%$ for jets with $E_T = 50$ and $E_T = 100$ GeV, respectively, and already at $R = 0.7$ the effect reduces to about 2%. However, one must be cautious about these findings, since this prediction has been calculated assuming a rather low value of the gluon density at LHC conditions. We have verified (without embedding in HIJING) that for $R = 0.7$ more than 90% of the energy remains in the jet cone. Up to 45% of the rise at jet energies lower than 50 GeV can be attributed to the contribution of the underlying heavy-ion background to the jet signal. Jet suppression (at fixed value of R) may be observed in the suppression of inclusive single-jet spectra in central nucleus–nucleus relative to peripheral or pp collisions. Analogous to eq. (1), we therefore define the nuclear modification factor for jets, $R_{AA}^{jet}(E_T, \eta; b)$, according to

$$R_{AA}^{jet}(E_T, \eta; b) = \frac{1}{\langle N_{coll}(b) \rangle} \times \frac{d^2 N_{AA}^{jet}/dE_T d\eta}{d^2 N_{pp}^{jet}/dE_T d\eta}. \quad (5)$$

Equation (5) implicitly depends on the (fixed) value of R used to find the jets. Figure 5 shows $R_{AA}^{jet}(E_T)$ for different quenching scenarios in 0–10% central Pb–Pb.

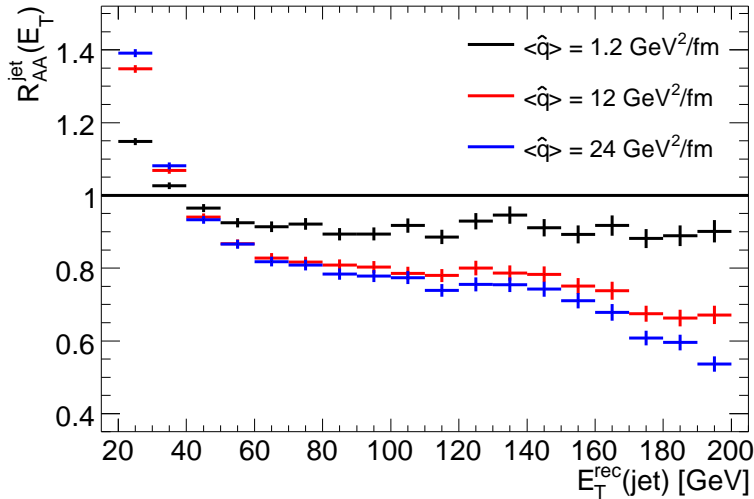


Figure 5. The nuclear modification factor for jets, $R_{AA}^{jet}(E_T)$, as a function of the reconstructed jet energy, E_T^{rec} , for different quenching scenarios in 0–10% central Pb–Pb. The jets in pp and Pb–Pb are identified with the cone finder using $R = 0.3$ and $p_T > 2$ GeV. (Full calorimetry is assumed.)

4.2. Longitudinal momentum modification factor

The signature of medium-induced gluon radiation should be visible in the modification of the jet fragmentation function as measured through the longitudinal and transverse momentum distributions of associated hadrons within the jet. The momenta parallel to the jet axis, $p_L = p_{\text{hadron}} \cos(\theta_{\text{jet}}, \theta_{\text{hadron}})$, are expected to be reduced (jet quenching), while the momenta in the transverse direction, $j_T =$

$p_{\text{hadron}} \sin(\theta_{\text{jet}}, \theta_{\text{hadron}})$, to be increased (transverse heating). In our simulation for technical reasons we can not give an explicit transverse-momentum kick to the radiated gluons. Therefore, we concentrate on the changes of the longitudinal fragmentation.

We define the longitudinal momentum modification factor according to

$$R_{AA}^{p_L}(p_L) = \frac{N_{pp}^{\text{jets}}}{N_{AA}^{\text{jets}}} \frac{dN_{AA}/dp_L}{dN_{pp}/dp_L} \quad (6)$$

where for proper normalization N_{AA}^{jets} and N_{pp}^{jets} account the total number of jets that were found in A–A and pp, respectively. Equation (6) implicitly depends on the transverse jet-energy range of jets taking into account in the distributions. Figure 6 shows $R_{AA}(p_L)$ for jets with reconstructed energies of $E_T^{\text{rec}} > 80$ GeV in 0–10% central Pb–Pb compared for the different quenching scenarios.

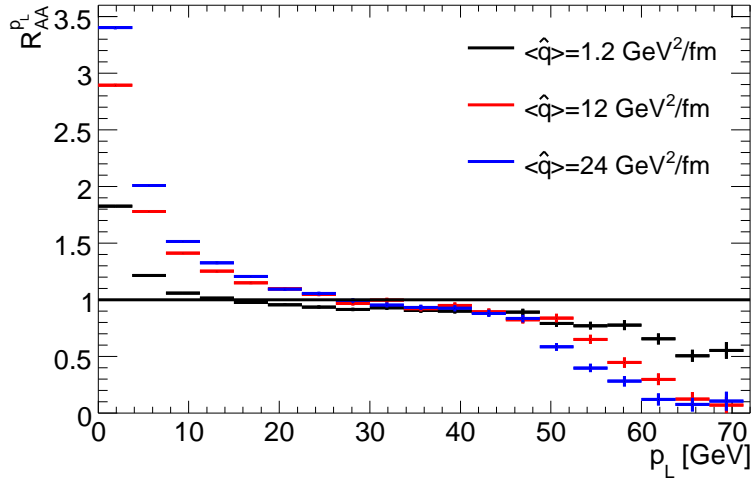


Figure 6. Longitudinal momentum modification factor, $R_{AA}^{p_L}$, for jets with $E_T^{\text{rec}} > 80$ GeV and different quenching scenarios in 0–10% central Pb–Pb. The jets in pp and Pb–Pb are identified with the cone finder using $R = 0.3$ and $p_T > 2$ GeV. (Full calorimetry is assumed.)

The expected behavior is clearly visible: higher medium density leads to stronger suppression for large longitudinal momenta and enhancing of smaller momenta. At low p_L the effect becomes most apparent. At these low momenta there is an moderate additional contribution from particles which belong to the underlying heavy-ion background, which amounts to about 20% for $p_L < 5$ GeV. It might be interesting to study the (average) slope of $R_{AA}(p_L)$ as a function of the reconstructed jet energy.

5. Conclusions

We have presented the PQM model [20] which is able to describe high- p_T suppression effects at RHIC. Its application to LHC conditions leads to the expectation that R_{AA} is essentially constant with p_T , also for very high momenta up to 100 GeV. The nuclear modification factor for leading hadrons is largely dominated by surface effects. This limits its sensitivity to the density of the created medium. The measurement of reconstructed jets above the underlying heavy-ion background may allow to probe the medium to deeper extents. In a simulation of jet quenching at LHC we have studied two observables: the nuclear modification factor for jets, R_{AA}^{jet} , and the nuclear modification factor for the longitudinal momenta of particles along the jet axis, $R_{AA}^{p_L}$. The definitions implicitly depend on the parameters used to find the jets. For jets with $E_T \gtrsim 50$ GeV both are suitable measures to quantify deviations from the pp case: $R_{AA}^{\text{jet}}(E_T)$ decreases with increasing E_T and $R_{AA}^{p_L}$ is enhanced at low p_L and suppressed

at high p_L . However, for jets with $E_T < 50$ GeV suffer from the contamination of the jet cone by uncorrelated particles from the underlying background which at these energies severely influences measured jet properties.

Acknowledgments

The author acknowledges fruitful discussions with A. Dainese, A. Morsch, G. Paic and R. Stock.

References

- [1] I. Arsene and others (BRAHMS). *Phys. Rev. Lett.*, 91:072305, 2003. [[arXiv:nucl-ex/0307003](#)].
- [2] J. Adams and others (STAR). *Phys. Rev. Lett.*, 91:172302, 2003. [[arXiv:nucl-ex/0305015](#)].
- [3] S.S. Adler and others (PHENIX). *Phys. Rev.*, C69:034910, 2004. [[arXiv:nucl-ex/0308006](#)].
- [4] S.S. Adler and others (PHENIX). *Phys. Rev. Lett.*, 91:072301, 2003. [[arXiv:nucl-ex/0304022](#)].
- [5] B.B. Back and others (PHOBOS). *Phys. Lett.*, B578:297–303, 2004. [[arXiv:nucl-ex/0302015](#)].
- [6] C. Adler and others (STAR). *Phys. Rev. Lett.*, 90:082302, 2003. [[arXiv:nucl-ex/0210033](#)].
- [7] J. Adams and others (STAR). *Phys. Rev. Lett.*, 93:252301, 2004. [[arXiv:nucl-ex/0407007](#)].
- [8] F. Wang (STAR). *J. Phys.*, G30:S1299–S1304, 2004. [[arXiv:nucl-ex/0404010](#)].
- [9] J. Adams and others (STAR). 2005. [[arXiv:nucl-ex/0501016](#)].
- [10] S.S. Adler and others (PHENIX). *Phys. Rev. Lett.*, 91:072303, 2003. [[arXiv:nucl-ex/0306021](#)].
- [11] J. Adams and others (STAR). *Phys. Rev. Lett.*, 91:072304, 2003. [[arXiv:nucl-ex/0306024](#)].
- [12] B.B. Back and others (PHOBOS). *Phys. Rev. Lett.*, 91:072302, 2003. [[arXiv:nucl-ex/0306025](#)].
- [13] X.N. Wang. *Phys. Rev.*, C61:064910, 2000. [[arXiv:nucl-th/9812021](#)].
- [14] X.-N. Wang. *Phys. Rev.*, C58:2321, 1998. [[arXiv:hep-ph/9804357](#)].
- [15] X.N. Wang. *Nucl. Phys.*, A702:238, 2002. [[arXiv:hep-ph/0208094](#)].
- [16] X.-N. Wang. *Phys. Lett.*, B579:299–308, 2004. [[arXiv:nucl-th/0307036](#)].
- [17] I. Vitev and M. Gyulassy. *Phys. Rev. Lett.*, 89:252301, 2002. [[arXiv:hep-ph/0209161](#)].
- [18] A. Adil and M. Gyulassy. *Phys. Lett.*, B602:52–59, 2004. [[arXiv:nucl-th/0405036](#)].
- [19] I. Vitev. *Phys. Lett.*, B606:303–312, 2005. [[arXiv:nucl-th/0404052](#)].
- [20] A. Dainese, C. Loizides, and G. Paic. *Eur. Phys. J.*, C38:461–474, 2005. [[arXiv:hep-ph/0406201](#)].
- [21] K.J. Eskola, H. Honkanen, C.A. Salgado, and U.A. Wiedemann. *Nucl. Phys.*, A747:511–529, 2005. [[arXiv:hep-ph/0406319](#)].
- [22] K. Gallmeister and W. Cassing. *Nucl. Phys.*, A748:241–259, 2004. [[arXiv:hep-ph/0408223](#)].
- [23] D. Hardtke and T.J. Humanic. *Phys. Rev.*, C71:034906, 2004. Erratum-ibid. C71 (2006) 039903 [[arXiv:nucl-th/0405064](#)].
- [24] C. Loizides. PhD thesis, University of Frankfurt, 2005. [[arXiv:nucl-ex/0501017](#)].
- [25] C.A. Salgado and U.A. Wiedemann. *Phys. Rev.*, D68:014008, 2003. [[arXiv:hep-ph/0302184](#)].
- [26] B. Müller. *Phys. Rev.*, C67:061901, 2003. [[arXiv:nucl-th/0208038](#)].
- [27] R. Baier, Y.L. Dokshitzer, A.H. Mueller, and D. Schiff. *JHEP*, 09:033, 2001. [[arXiv:hep-ph/0106347](#)].
- [28] U.A. Wiedemann. *Nucl. Phys.*, A690:731–751, 2001. [[arXiv:hep-ph/0008241](#)].
- [29] C.A. Salgado and U.A. Wiedemann. *Phys. Rev. Lett.*, 93:042301, 2004. [[arXiv:hep-ph/0310079](#)].
- [30] T. Sjöstrand and others. *Comput. Phys. Commun.*, 135:238, 2001. [[arXiv:hep-ph/0010017](#)].
- [31] A. Morsch (ALICE). *J. Phys. G: Nucl. Part. Phys.*, 31:1–6, 2005.
- [32] M. Gyulassy and X.N. Wang. *Comput. Phys. Commun.*, 83:307–331, 1994.
- [33] G.C. Blazey and others. 2000. [[arXiv:hep-ex/0005012](#)].